Journal of Applied Electrochemistry **29**: 1329–1338, 1999.

Zirconium and Ebonex® as cathodes for sulphite ion oxidation in sulphuric acid

K. SCOTT*, H. CHENG and W. TAAMA
Department of Chemical & Process Engineering, University of Newcastle upon Tyne, Merz Court, Newcastle upon Tyne, NE1 7RU
*(*author for correspondence, fax: +44 191 2611182)*

Received 15 December 1998; accepted in revised form 2 June 1999

Key words: anodic oxidation, Ebonex®, lead dioxide anode, sulphur dioxide, sulphuric acid recycling, zirconium

Abstract

The electrochemical behaviour of zirconium metal and Ebonex® cathodes during the electrolysis of sulphite ions in sulphuric acid, at temperatures from 20 to 90 °C, is reported. The inactivity of these materials for the reduction of sulphite ions to sulphur is demonstrated, making the undivided cell oxidation of sulphite ions to sulphuric acid, at concentrations greater than 3.0 mol dm^{-3}, a viable process. The use of these two cathodes materials in conjunction with lead dioxide-coated and palladium oxide-coated anodes for sulphite ion oxidation is described. Linear sweep voltammograms, chronopotentiometry and batch electrolysis data are presented for sulphite ion oxidation and demonstrate the concept of an undivided electrolysis for the oxidation of sulphur dioxide in sulphuric acid.

1. Introduction

The removal of sulphur dioxide from waste and process gases is of industrial importance and can be achieved by direct and indirect oxidation and by indirect reduction [1]. Indirect reduction typically produces elemental sulphur whereas oxidation can produce sulphuric acid or other products such as dithionite ion. Indirect oxidation involves the generation of species, such as bromine, which raises other environmental issues associated with, for example, disposal of spent bromide or its reoxidation to bromine. Direct oxidation has previously been performed in membrane electrolysers to avoid the formation of elemental sulphur, at the cathode, which deactivates the system. An undivided cell electrolysis, which can operate without cathodic sulphur formation, is potentially an attractive alternative to a divided cell electrolysis in terms of lower cell cost, lower reactor installation cost and lower energy consumption. The process for the treatment of SO_2, in the absence of oxygen, is based on the following electrode reactions:

$$SO_3^{2-} + 2\,H_2O = SO_4^{2-} + 2\,H^+ + 2\,e^-$$

$$2\,H^+ + 2\,e^- = H_2$$

To achieve successful undivided cell oxidation of sulphite ions, or dissolved sulphur dioxide, in sulphuric acid we identified two candidate electrode materials: zirconium metal and Ebonex®. Ebonex® is a proprietary conductive ceramic material comprised of Magneli phase suboxides of titanium dioxide. The material is chemically stable and corrosion resistant material with a similar electrical conductivity to graphite. It has, consequently, attracted significant interest as an electrode material for electrocatalytic coatings. A review of the properties and applications of Ebonex has very recently been published [2]. In applications as a substrate for coated anodes Ebonex® exhibits superior resistance to corrosion than either titanium or niobium in the presence of hydrochloric acid, sulphuric acid, nitric acid and fluoride ions [3]. As a cathode material for hydrogen evolution it is not susceptible to hydride formation, thus making it a potentially useful material as a bipolar electrode in circumstances where hydrogen gas is evolved. Voltammetry data at Ti_nO_{2n-1} ceramic electrodes close to the potential for hydrogen evolution has been reported [4]. In 10% sulphuric acid the electrode exhibits approximately Tafel-like behaviour, for the hydrogen evolution reaction, with a slope of approximately 100 mV $decade^{-1}$. For Ti_4O_7 the electrochemical behaviour varies with the material porosity. More porous material (with 80% of pores >1 μm) exhibits significantly higher current densities, at a given potential, than less porous varieties [pore size 0.1 μm].

Ebonex® and lead dioxide coated Ebonex® have been investigated for the anodic production of ozone from fluoroboric acid [5]. Performance of uncoated Ebonex® was poor for ozone production, $<0.6\%$ current efficiency, with oxygen evolution and later corrosion of the material, the major reaction processes. The PbO_2-coated Ebonex® however, showed significantly better performance for ozone generation ($\sim$5% to 15% current efficiency for ozone) and negligible corrosion of the substrate, primarily due to lower potentials (by around 500 mV) on the coated material compared to those on uncoated Ebonex®. Coated Ebonex® anodes are, in

terms of material stability, potentially suitable materials for oxidations.

Performing undivided cell electrolysis rather than divided cell electrolysis, using membranes, is attractive for several reasons, for example, reduced cell cost, power supply cost and energy consumption, and is economically desirable in many cases. Effective operation requires identification of suitable counter electrodes which do not interfere with the desired synthesis reaction. Generally, this will involve reactions at the counter electrode which are independent of the desired reaction (e.g., reactions of the solvent), that is, hydrogen and oxygen evolution or use consumable anodes. Several examples of replacing a divided cell operation with an undivided cell operation have been applied commercially, notably the synthesis of adiponitrile from acrylonitrile [6], where electrolyte and anode were selected to promote oxygen evolution. Other applications of the concept for electrosynthesis have been tried, for example, in glyoxylic acid synthesis, with coated metal anodes [7] and in synthesis with zirconium [8]. In the latter case, zirconium was used as an anode for oxygen evolution during electrosynthesis due to its lack of electrocatalytic activity for the reagents used, thus enabling an undivided electrolysis to proceed with high product yield.

In this paper we present polarisation data from the use of several materials as cathodes during sulphite ion oxidation. Data are also reported for sulphite ion oxidation on lead dioxide coated electrodes and on a commercial palladium oxide coated electrode. It is also expected that the results of this work will lead to viable bipolar electrodes for the oxidation of SO_2 to sulphuric acid in an undivided cell.

2. Experimental details

Experiments were performed in a sealed, magnetically stirred H-type glass cell, 250 cm^3 in volume. All electrodes had surface areas of 1.0 cm^2. The anode materials used were lead dioxide-coated platinum, titanium and Ebonex® and palladium-coated titanium (Electrocatalytic Inc., USA). The cathodes were zirconium metal (Goodfellow Metals), Ebonex® (Altraverda Ltd), tantalum, titanium, nickel, stainless steel, graphite and glassy carbon. Two grades of Ebonex® were used a porous material (20% porosity) and a nonporous material (4% porosity). The lead dioxide anodes were prepared by electrodeposition of PbO_2, onto the substrate foil, from a solution of lead nitrate (200 g dm^{-3}) and nitric acid (5 g dm^{-3}) at 65 °C and at a current density of 25 mA cm^{-2} for 15 min. The lead dioxide deposits had a density of 9.3 g cm^{-3} and thickness of 13 μm.

Electric power to the batch cell was supplied by a computer controlled Versastat manufactured by EG&G (PAR). Electrolyte solutions were typically 0.05 mol dm^{-3} sulphuric acid which were deoxygenated prior to use. Linear sweep voltammetry (LSV), chronopotentiometry and preparative batch experiments were performed with this cell. All potential scan rates were 100 mV s^{-1} unless otherwise stated. Preparative electrolyses were carried out galvanostatically at current densities in the range of 5–25 mA cm^{-2}, at 20 °C and atmospheric pressure. The cell solution was sealed and magnetically stirred with off gases passed through iodine traps to determine vapour losses of SO_2. The losses of SO_2 from the solution were also assessed by performing gas stripping runs without electrolysis. Current efficiencies were calculated on the basis of concentration differences of SO_3^{2-} in solution with correction for the loss in the gas/vapour from the cell. In addition, the increase in acid concentration at the end of electrolysis was determined volumetrically and correlated reasonably accurately (±20%) with the change in sulphite concentration. The sulphite concentration was determined iodimetrically immediately before and after each individual set of LSV experiments. The variation in concentration of SO_3^{2-} over each set of experiments was within 6% of the mean concentration of 0.05 mol dm^{-3}. Steady state current density, electrode potential curves were obtained using chronopotentiometry at 20 °C.

Prior to each run, electrodes were washed with dilute sulphuric acid and then rinsed in doubly distilled water. Anodes were pre-treated anodically at 0.3 V for 5 min in the electrolyte solution prior to commencing each preparative experiment. Cathodes were pretreated by holding the potential at 0.2 V vs SCE for 5 min and performing a cathodic sweep at a rate of 20 mV s^{-1}.

3. Results and discussion

3.1. *Evaluation of cathode materials*

An objective of this study was to investigate suitable cathode materials which, during the undivided cell oxidation of sulphite, do not cathodically reduce sulphite to sulphur. LSV was performed on a range of materials; Ebonex® (porous and nonporous), zirconium, tantalum, titanium, nickel, stainless steel, natural graphite and glassy carbon. The influence of temperature, sulphuric acid concentration and sulphite concentration were investigated.

Preliminary screening of cathode materials was performed using nickel, stainless steel, natural graphite and glassy carbon. Linear sweeps voltammetry was performed at 20 °C using an electrolyte solution of 0.05 mol dm^{-3} sodium sulphite in 3.0 mol dm^{-3} sulphuric acid. The LSV data (Figure 1) typically shows that these four materials, as anticipated, are active towards the reduction of sulphite ions to sulphur, exhibiting a pre-reduction wave before hydrogen evolution. These reduction waves started at potentials in the range −0.1 to −0.5 V vs SCE depending upon the material.

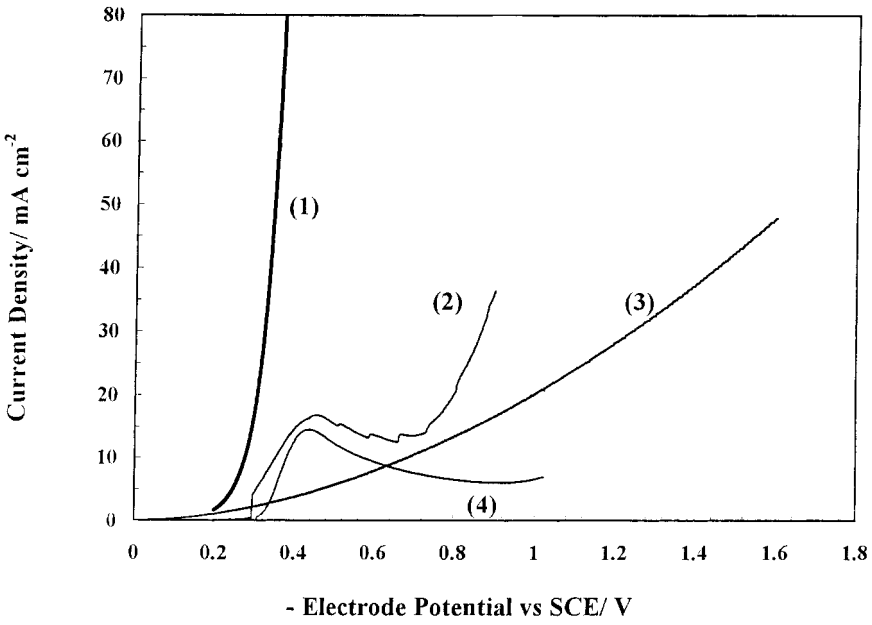

Fig. 1. Linear sweep voltammograms for nickel, stainless steel, natural graphite and glassy carbon cathodes in sodium sulphite, sulphuric acid electrolyte. 20 °C, 0.5 mol dm^{-3} SO_3^{2-}, 3.0 mol dm^{-3} sulphuric acid. Sweep rate 100 mV s^{-1}. Key: (1) nickel, (2) natural graphite, (3) glassy carbon and (4) stainless steel.

Background scans performed with 3.0 mol dm^{-3} sulphuric acid did not exhibit a reduction wave at −0.25 V vs SCE. The formation of elemental sulphur was visible for all the four electrode materials and generally affected the reproducibility and characteristics of the curves on repeated scans. The scans frequently exhibited a rapid increase in current at the onset of reduction followed by some oscillatory behaviour, in the hydrogen evolution region, at higher potentials, as seen in the wave for graphite in Figure 1.

Linear sweep voltammograms at 100 mV s^{-1} for zirconium, tantalum and Ebonex® (porous and nonporous) are shown in Figure 2 for solutions of 0.5 mol dm^{-3} sulphuric acid with 0.05 mol dm^{-3} sodium sulphite. The data for zirconium (Figure 2(a)) shows a relatively slow rise of current density with potential. The LSV data for zirconium with and without sulphite ions are similar and do not indicate any significant reduction of sulphite. The formation of elemental sulphur was not observed with this cathode material. The LSV data for the porous grade of Ebonex® with and without sulphite ions are shown in Figure 2(b). The onset of electrode activity occurs at lower potentials in the presence of sulphite. The generation of hydrogen gas becomes significant at potentials of −0.4 V vs SCE which are significantly higher (less negative) than those for zirconium. At higher potentials the LSV data with and without sulphite present are similar. As with zirconium, no sulphur formation was observed. The LSV data for tantalum in sulphuric acid is similar to that of Ebonex®, exhibiting a reduction wave for hydrogen evolution which starts at −1.0 V vs SCE and rises relatively fast with potential in comparison to zirconium. In the presence of sulphite the LSV data for Tantalum (Figure 2(c)) is noticeably different to that of zirconium and Ebonex® cathodes. Sulphur formation was observed using tantalum cathodes in some, but not all, scans. From this limited data the use of tantalum was not progressed further. However Ebonex® and zirconium would appear to be suitable cathode materials for undivided cell oxidation of sulphur dioxide.

The electrochemical behaviour of the smooth nonporous Ebonex® cathode in 3.0 mol dm^{-3} sulphuric acid (Figure 3) is similar to that of porous Ebonex and zirconium cathodes. Overpotentials for hydrogen evolution are greater on nonporous Ebonex® than on porous Ebonex®. In the range of 5–50 mA cm^{-2} the change in electrode potential for porous and nonporous Ebonex are only marginally different, porous Ebonex® 1.0 V decade^{-1} (cf. nonporous Ebonex® 1.075 V decade^{-1}). In the presence of sulphite, the current density vs potential responses of both Ebonex cathodes are again similar and sulphur formation is not observed.

The effect of sulphuric acid concentration on the LSV curves for porous Ebonex® is shown in Figure 3. At a fixed potential the current density increases significantly with concentration, demonstrating the benefit, in terms of reduced cell voltage, of using, and thus producing, high concentrations of acid from sulphur dioxide oxidation.

Figure 4 shows the effect of temperature on the LSV curves for Ebonex® cathodes. Higher temperatures result in higher current densities at fixed potentials, over the range 20–90 °C. The data at the higher temperature of 90 °C will inevitably be affected by a reduced concentration of sulphite in solutions due to vaporisation and loss in the hydrogen exit gas.

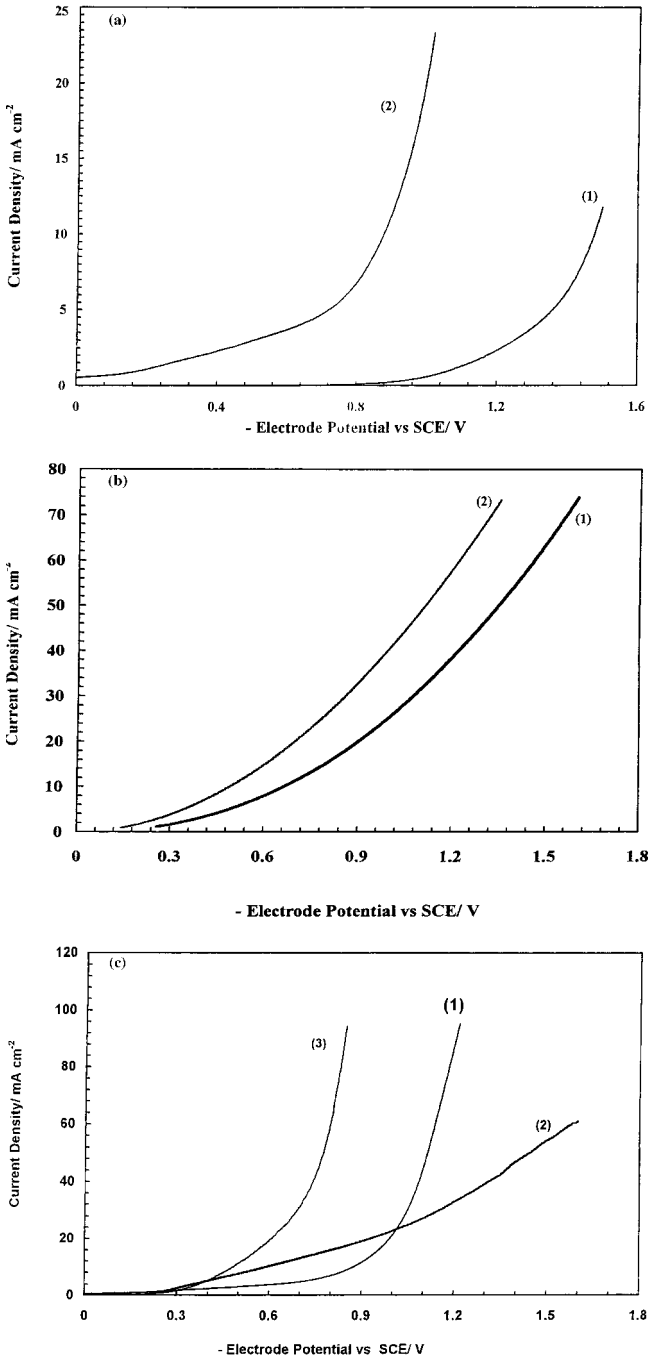

Fig. 2. Linear sweep voltammograms for zirconium, tantalum and Ebonex® cathodes. 20 °C, 3.0 mol dm^{-3} sulphuric acid. Sweep rate 100 mV s^{-1}. (a) Zirconium: (1) sulphuric acid and (2) sulphuric acid and 0.5 mol dm^{-3} SO_3^{2-}. (b) Ebonex®: (1) sulphuric acid and (2) sulphuric acid and 0.5 mol dm^{-3} SO_3^{2-}. (c) Zirconium: (1) Ebonex® (2) and tantalum (3) sulphuric acid and 0.5 mol dm^{-3} SO_3^{2-}.

3.2. *Anodic oxidation of sulphite*

Oxidation of sulphite ions in sulphuric acid was studied using lead dioxide coated platinum and titanium and palladium oxide-coated titanium electrodes.

Figure 5 shows LSV curves for a lead dioxide coated platinum electrode. An oxidation peak at 900 mV vs SCE in the presence of the sulphite ions indicates oxidation of that species. There is no background oxidation peak with sulphuric acid in the absence of sulphite ions. In view of the oxidation of sulphite at lead dioxide, the use of lead dioxide coated titanium and Ebonex® were investigated as potential electrodes for bipolar cell operation.

A series of cyclic voltammograms, for lead dioxide coated titanium is shown in Figure 6 for the oxidation of 0.05 mol dm^{-3} SO_3^{2-} in 0.5 mol dm^{-3} sulphuric acid. There is a major oxidation current peak between 850–1000 mV. This peak current becomes broader and increases in height with the anodic sweep rate. The peak current varies with the root of the potential sweep rate (Figure 7) which, suggests that a diffusion controlled process is involved in an irreversible oxidation of sulphite ions. However, the plot does not go through the origin: this indicates that the process is not a simple mass transport controlled event. At low potential scan rates, several oxidation peaks are observed indicating the complex process of sulphite ion oxidation at lead dioxide coated titanium substrates. Notably a second oxidation peak appears at more positive potentials at around 1200 mV. In addition, several smaller peaks or shoulders also appear on forward and reverse scans. In the oxidation of sulphite there are several processes occurring including (i) sulphite ion diffusion from the bulk electrolyte and through the PbO_2 film onto the inner surface of the film and the Ti substrate, (ii) direct oxidation of sulphite to sulphate, (iii) reaction of sulphite species with the oxide surface followed by oxidation of lead sulphate to lead dioxide, (iv) sulphate ion diffusion, (v) sulphate ion diffusion through the film and from the surface. The above processes, together with a pseudo capacitance behaviour, therefore can lead to a complex voltammogram characteristic at low scan rates. At faster scan rates, the oxidation and/or adsorption of species is inhibited by diffusion of sulphite species at the surface.

Steady state current density, electrode potential curves were produced for lead dioxide coated titanium anodes using chronopotentiometry at 20 °C. Very stable potentials were achieved, at fixed current densities, for the reaction on lead dioxide. The data shown in Figure 8 exhibits Tafel behaviour with a transfer coefficient of 0.057 (Tafel slope 513 mV decade^{-1}) and exchange current density of 0.0123 mA cm^{-2}. The value of exchange current density assumes a simple irreversible two-electron transfer although for sulphite oxidation this is unlikely to be the case. A previous study of SO_2 oxidation in 0.1 mol dm^{-3} Na_2SO_4 electrolyte on lead dioxide using a rotating disc electrode indicated that SO_2 oxidation occurs mainly by an oxide mechanism involving the lead dioxide/lead surface [10]:

$$SO_3^{2-} \rightarrow SO_3^{2-*} \quad (1)$$

$$SO_3^{2-*} + PbO_2 + 2\,H^+ \rightarrow PbSO_4 + H_2O \quad (2)$$

$$PbSO_4 + 2\,H_2O \rightarrow PbO_2 + SO_4^{2-} + 4\,H^+ + 2\,e^- \quad (3)$$

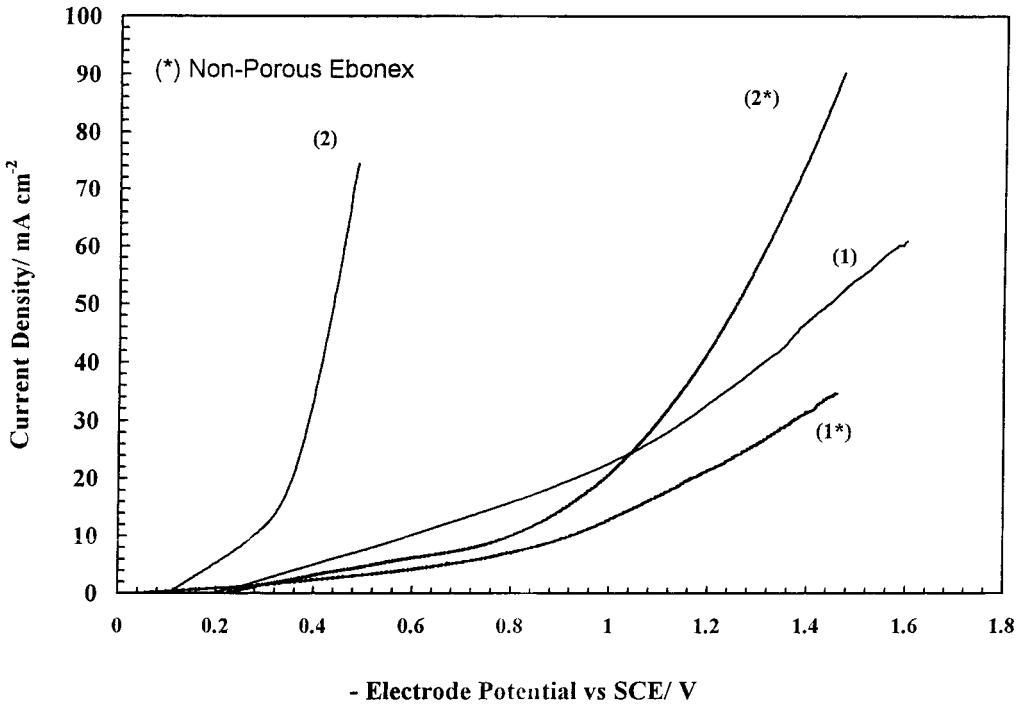

Fig. 3. Effect of sulphuric acid concentration on linear sweep voltammograms for non-porous Ebonex® (∗). 50 °C, 0.5 mol dm^{-3} SO_3^{2-}. Sweep rate 100 mV s^{-1}. Key: (1) 0.5 mol dm^{-3} sulphuric acid and (2) 3.0 mol dm^{-3} sulphuric acid.

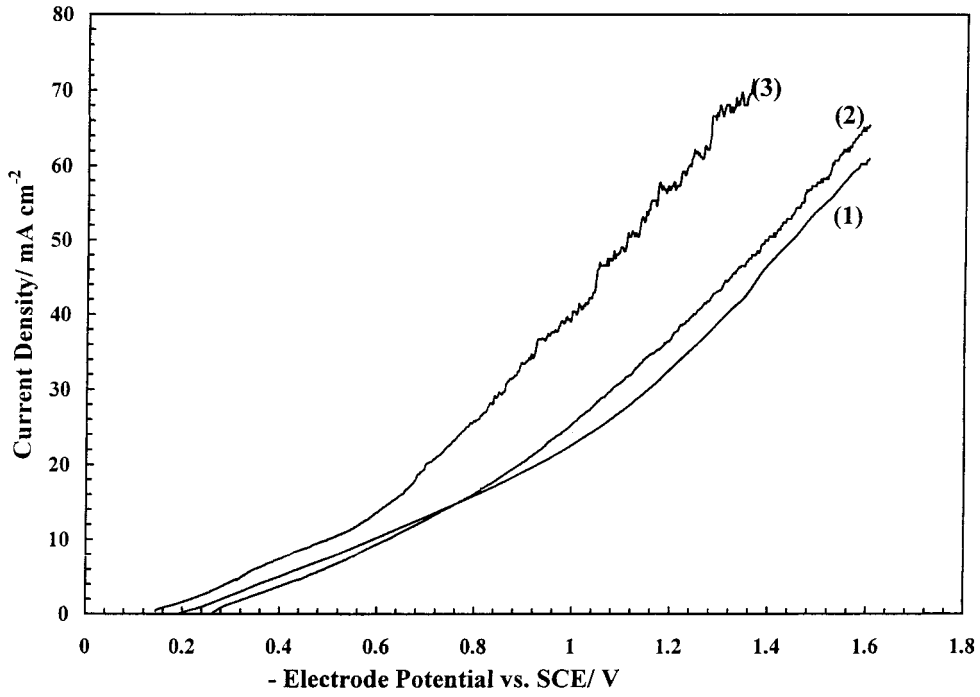

Fig. 4. Effect of temperature on the linear sweep voltammograms of Ebonex® 0.5 mol dm^{-3} SO_3^{2-}, 3.0 mol dm^{-3} sulphuric acid. Sweep rate 100 mV s^{-1}. Key: (1) 20 °C, (2) 50 °C and (3) 90 °C.

This mechanism differs from that at platinum under similar conditions, where a direct oxidation mechanism is suggested as dominant [10]:

$$SO_3^{2-} \rightarrow SO_3^{2-*} \quad (1)$$

$$SO_3^{2-*} + H_2O \rightarrow SO_4^{2-} + 2H^+ + 2e^- \quad (4)$$

It is claimed that a direct mechanism also contributes, to a small extent, towards SO_2 oxidation at lead dioxide electrodes. The transfer coefficients obtained, using a five parameter model, were 0.2 for Reaction 3 and 2 and 0.187 for Reaction 4.

The value of Tafel slope observed for sulphite ion oxidation at lead dioxide is high in comparison to

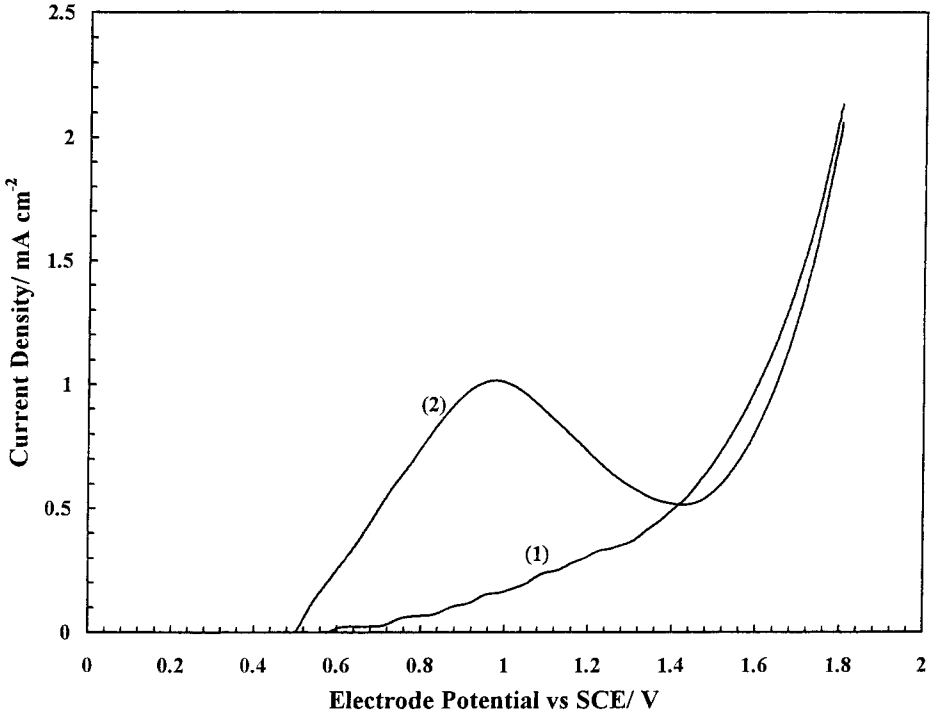

Fig. 5. Linear sweep voltammogram for lead dioxide coated titanium anodes. 20 °C, 0.5 mol dm^{-3} SO_3^{2-}, 3.0 mol dm^{-3} sulphuric acid. Sweep rate 50 mV s^{-1}.

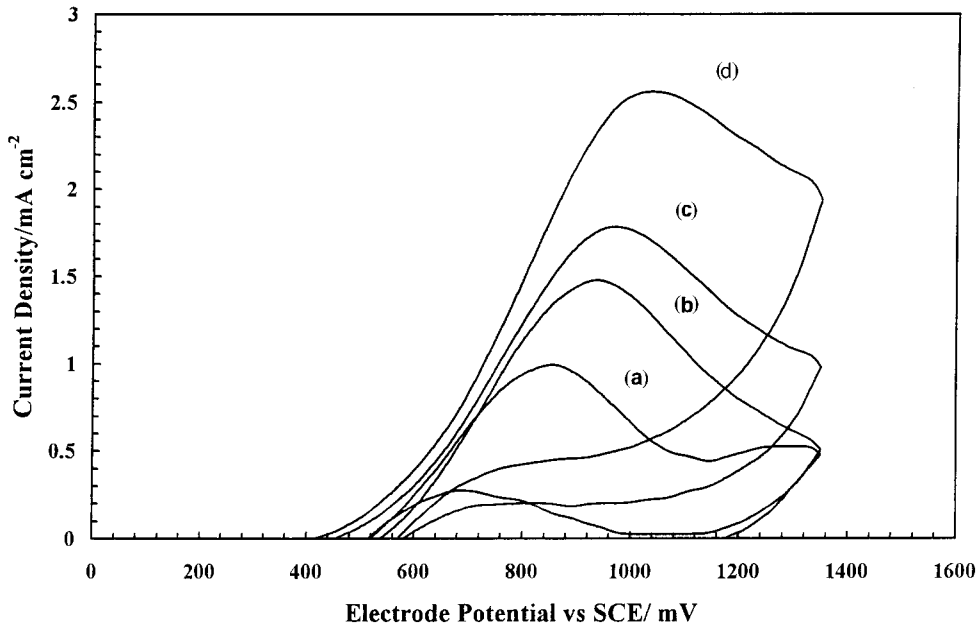

Fig. 6. Cyclic voltammograms for lead dioxide coated titanium anodes. 0.5 mol dm^{-3} SO_3^{2-}, 3.0 mol dm^{-3} sulphuric acid. Sweep rates: (a) 50, (b) 100, (c) 200 and (d) 500 mV s^{-1}.

previously published values [9] for noble metals based on a simple Tafel equation. A Tafel slope of 54 mV decade^{-1} was obained by Lu and Ammon [9] on palladium for a 2.0 mol dm^{-3} sulphur dioxide in a 50 wt% aqueous sulphuric acid solution. However, reported values of Tafel slope for graphite and glassy carbon are significantly higher: 402 and 460 mV decade^{-1}, respectively, in 0.5 mol dm^{-3} sulphuric acid [11], 280 mV decade^{-1} for graphite [12], 410 mV decade^{-1} for graphite [13] in sodium sulphate, 280 mV decade^{-1} on glassy carbon [14] in 0.1 mol dm^{-3} sulphuric acid. Overall the sluggish activation of sulphite ion oxidation on graphite is duplicated on lead dioxide.

In view of the above demonstrated performance for sulphite ion oxidation, batch electrolysis was performed.

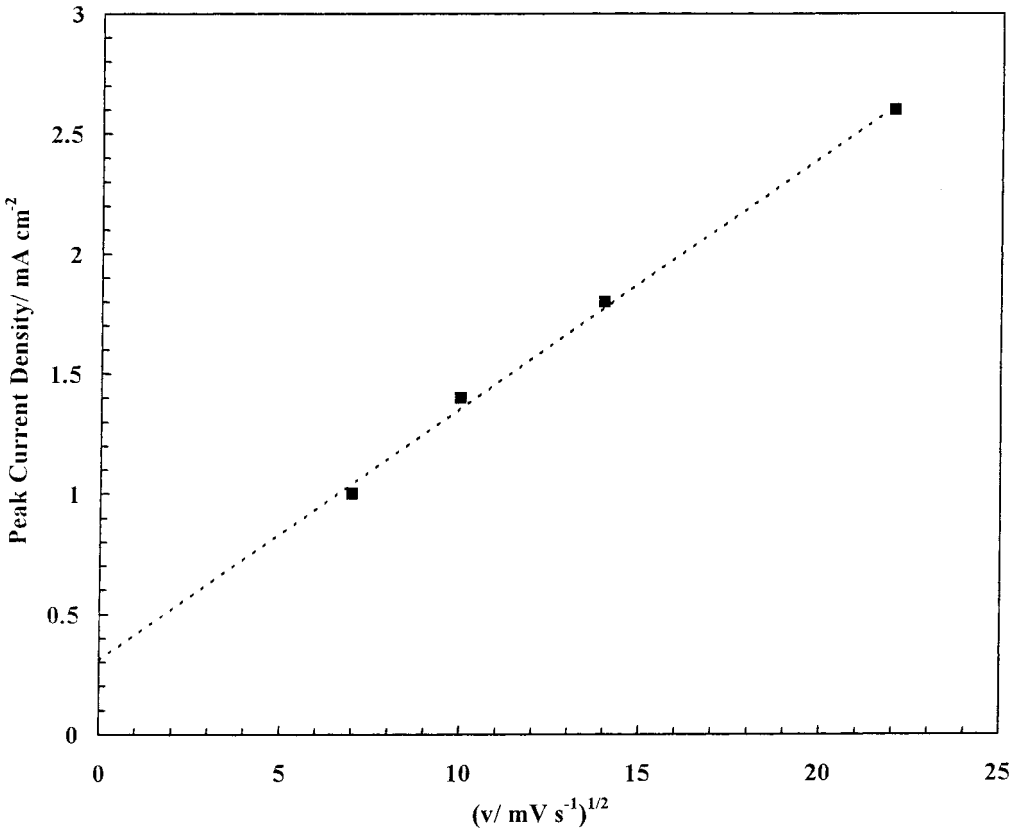

Fig. 7. Variation in peak current density with sweep rate for sulphite ion oxidation on lead dioxide coated titanium. 0.5 mol dm^{-3} SO_3^{2-}, 3.0 mol dm^{-3} sulphuric acid.

3.3. *Batch electrolysis*

To determine the efficiency of lead dioxide as an anode for sulphur dioxide oxidation, batch electrolyses were performed with solutions of nominal composition 0.045 mol dm^{-3} Na_2SO_3 in 2 mol dm^{-3} H_2SO_4 solutions. The cell was sealed and magnetically stirred with off gases passed through iodine traps to determine vapour losses of SO_2. The cathode material was Ebonex®.

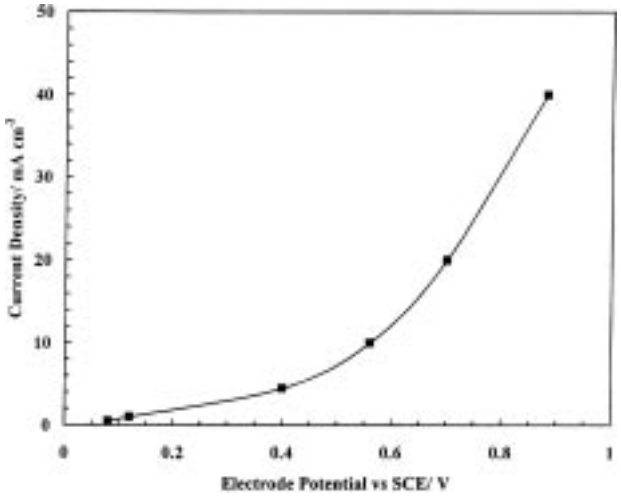

Fig. 8. Steady state electrode potential, current density behaviour for sulphite ion oxidation on lead dioxide coated titanium. 20 °C, 0.5 mol dm^{-3} SO_3^{2-}, 3.0 mol dm^{-3} sulphuric acid.

Figure 9 shows a typical result of electrolysis, at a current density of 10 mA cm^{-2}. At 20 °C, the current efficiency is initially high, greater than 95% and decreases as the concentration of sulphite falls due to oxidation. After 120 min electrolysis the overall current efficiency has fallen to 43% at a concentration of 0.035 kmol m^{-3}. The loss in current efficiency is due to the anodic oxidation of oxygen. The presence of oxygen in solution is also likely to result in the cathodic reduction of O_2 which may also generate peroxide species which could oxidise sulphite ions. Overall the variation of the sulphite ion concentration with time follows a simple exponential decay, which indicates that the oxidation of sulphite is under mass transport control with an approximate constant mass transport coefficient at the anode. The current efficiencies for sulphite ion oxidation on lead dioxide are comparable to those previously reported for platinised titanium and graphite [11].

At a temperature of 70 °C current efficiencies are lower than at 20 °C (Figure 10). Current efficiency is initially 67% at a starting concentration of 0.03 mol dm^{-3} and falls to 22% at a concentration of 0.0125 mol dm^{-3}. There was some difficulty in cell operation at a temperature of 70 °C, and above, as more SO_2 is stripped from solution. The accuracy of the data is ±10%, as seen in repeated runs. Overall, in the oxidation of sulphite solutions, lower temperatures are preferred, especially for solutions formed by absorbing SO_2 from the gas phase, as lower temperatures favour

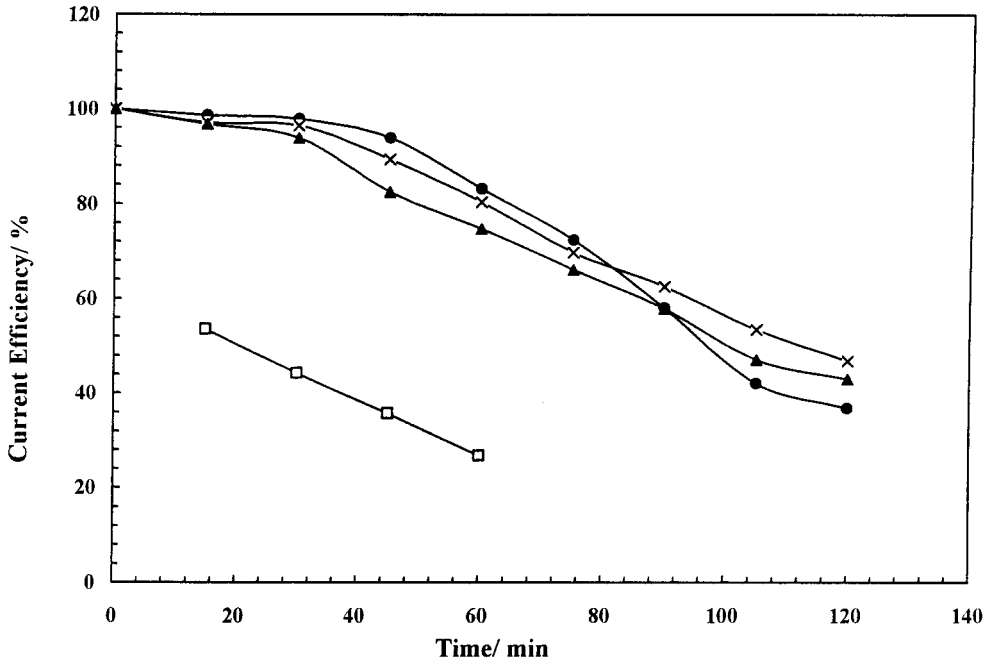

Fig. 9. Variation in current efficiency for sulphite ion oxidation on lead dioxide-coated titanium (▲), platinized titanium (×), graphite (●) and palladium oxide (□) coated titanium 20 °C. 0.5 mol dm^{-3} SO_3^{2-}, 3.0 mol dm^{-3} sulphuric acid.

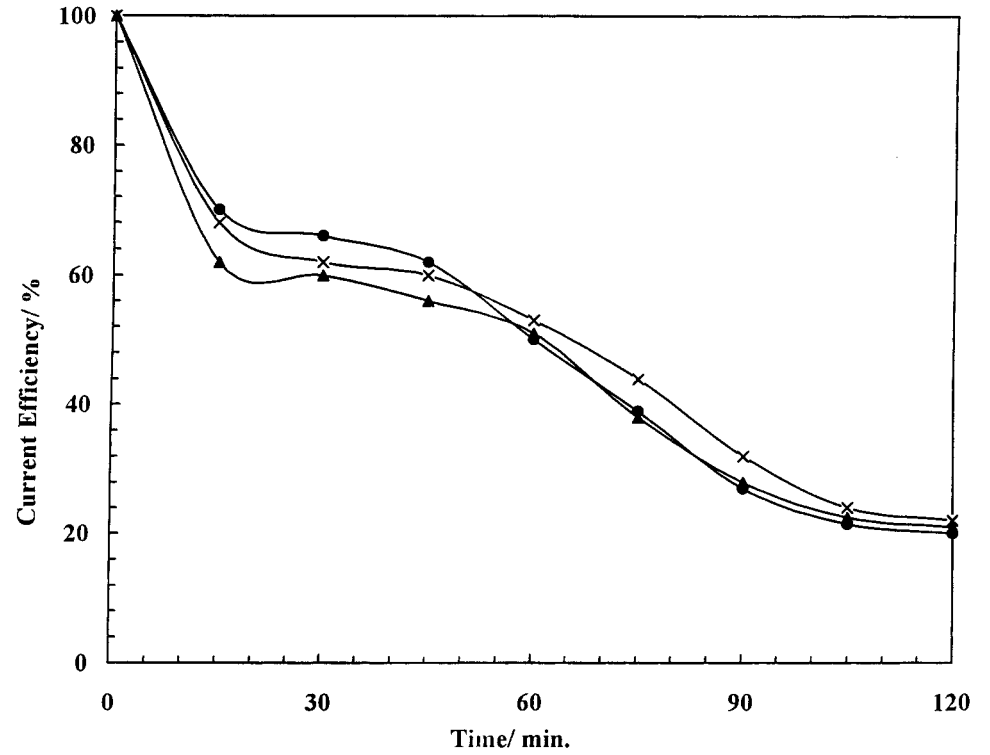

Fig. 10. Variation in current efficiency for sulphite ion oxidation on lead dioxide coated titanium (▲), platinized titanium (×) and graphite (●). 70 °C, 0.5 mol dm^{-3} SO_3^{2-}, 3.0 mol dm^{-3} sulphuric acid.

SO_2 solubility. The performance of the batch electrolysis with a Zr cathode was generally similar to that with an Ebonex® cathode in terms of current efficiencies and cell voltages.

Cell voltages measured in the batch cell were 2.5 and 2.3 V, respectively, at 20 and 70 °C, giving energy consumption, at the start of electrolysis, of approximately 2.5 kW h kg^{-1}. No material degradation of the lead dioxide anodes was observed over the series of repeated tests. In the case of graphite there are problems of electrode corrosion if operation is at potentials where excessive oxygen evolution occurs.

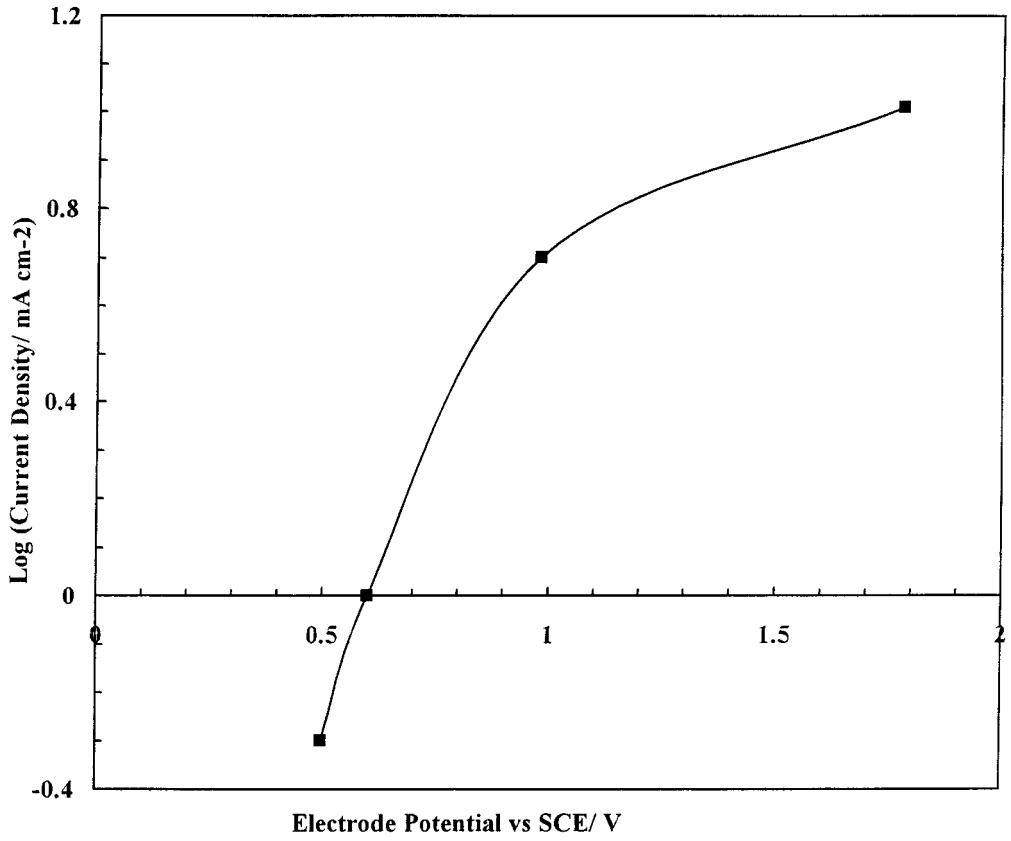

Fig. 11. Current density, potential behaviour for palladium oxide coated titanium obtained by chronopotentiometry. 20 °C, 0.5 mol dm^{-3} SO_3^{2-}. 3.0 mol dm^{-3} sulphuric acid.

3.3.1. *Palladium oxide coated anode*

In previous research we showed, using voltammetry, that palladium and palladium-coated electrodes, which were preanodized, were suitable for the anodic oxidation of sulphite in sulphuric acid [11]. However the preparation method used did not produce a good adherent deposit on the substrates used. Palladium oxide anodes have been previously reported to be suitable for oxidation of sulphite by Lu and Ammon [9]. We thus evaluated two commercial palladium oxide coated titanium electrodes (Electrocatalytic) for sulphite ion oxidation. Linear sweep voltammogramms on these electrodes were not reproducible and provided no real evidence for sulphite ion oxidation. This behaviour contrasts with that of oxidized palladium, where a distinct wave for sulphite oxidation is produced at 0.4 V vs SCE with a peak current density of 17 mA cm^{-2} [11]. The commercial palladium oxide electrode was unable to support significant current densities during oxidation. Chronopotentiometry (Figure 11) performed on this electrode, after LSV, also showed little activity for sulphite ion oxidation with a current density of 10 mA cm^{-2} achieved at 3.0 V vs SCE. The performance of palladium oxide for SO_2 oxidation was evaluated in batch electrolysis at constant current (10 mA cm^{-2}) (see Figure 9) Current efficiencies were approximately 50% at the start of electrolysis and fell significantly with time. Overall this indicates that although palladium oxide can oxidise sulphite ions, its use as a practical anode material is limited.

4. Conclusions

This research has demonstrated that the oxidation of sulphite ion in sulphuric acid can be performed in undivided cells using either Ebonex® or zirconium as cathodes. Both these cathodes do not reduce sulphite ions to sulphur under the conditions used.

The anodic oxidation of sulphur dioxide can be efficiently performed on lead dioxide coated titanium anodes. High current efficiencies, up to 100%, are achievable without the formation of elemental sulphur. Lead dioxide, characterised by good electrical conductivity and high oxygen overpotential, is able to withstand prolonged electrolysis at high anode potentials and is more effective than graphite. In terms of cost it is preferable to platinised anodes. Lead dioxide can be effectively plated onto Ebonex® to form a viable bipolar electrode material for electrochemical oxidation of SO_2.

Acknowledgement

The EPSRC supported W. Taama with a postdoctoral award during this study. Atraverda and Electrocatalytic supplied electrode materials.

References

1. K. Scott., 'Electrochemical Processes for Clean Technology' (RSC, Cambridge 1995).
2. J.R. Smith, F.C. Walsh and R.L. Clarke, *J. Appl. Electrochem.* **28** (1998) 1021.
3. K. Kendall, J.D. Birch, A.N. McAlford and R.L. Clark, 'Advanced Ceramics in Chemical Process Engineering', edited by B.C.H. Steele and D.P. Thompson. Proceedings of the British Ceramic Soc. No. 43 (1988) 131.
4. J. Przyluski and K. Kolbrecka, *J. Appl. Electrochem.* **23** (1993) 1063.
5. J.E. Graves, D. Pletcher, R.L. Clarke and F.C. Walsh, *J. Appl. Electrochem.* **22** (1992) 200.
6. K. Scott and B. Hayati, *Chem. Eng. and Proc.* **32** (1993) 253.
7. K. Scott, *Electrochim. Acta* **35** (1990) 621.
8. Y. Malherbe and C.H. Comninellis *J. App. Electrochem.* **24** (1994) 584.
9. P.W. Lu and R.L. Ammon, *J. Electrochem. Soc.* **127** (1980) 2610.
10. G. Kreysa and A. Storck, 'Electrochemical Cell Design and Optimisation Procedures', Dechema Monograph (VCH Verlagsgesellsehaft) Vol. **123** (1991) 225.
11. K. Scott and W. Taama in press Electrochimica Acta.
12. I.P. Voroshilov, N.N. Nechiporenko and E.P. Voroshilova, *Elektrokhimiya* **10** (1974) 1378.
13. T. Hunger, F. Lapicque and A. Storck, *J. Appl. Electrochem.* **21** (1991) 588.
14. G. Kreysa, J.M. Bisang, W. Kochanek and G. Linzbach, *J. Appl. Electrochem.* **15** (1985) 639.